Finite difference simulations of seismic wave propagation for understanding earthquake physics and predicting ground motions: Advances and challenges

Hideo Aochi, Thomas Ulrich, Ariane Ducellier, Fabrice Dupros, David Michéa

Finite difference simulations of seismic wave propagation for understanding earthquake physics and predicting ground motions: Advances and challenges

Hideo Aochi, Thomas Ulrich, Ariane Ducellier, Fabrice Dupros and David Michea

Bureau de Recherches Géologiques et Minières

h.aochi@brgm.fr

Abstract. Seismic waves radiated from an earthquake propagate in the Earth and the ground shaking is felt and recorded at (or near) the ground surface. Understanding the wave propagation with respect to the Earth's structure and the earthquake mechanisms is one of the main objectives of seismology, and predicting the strong ground shaking for moderate and large earthquakes is essential for quantitative seismic hazard assessment. The finite difference scheme for solving the wave propagation problem in elastic (sometimes anelastic) media has been more widely used since the 1970s than any other numerical methods, because of its simple formulation and implementation, and its easy scalability to large computations. This paper briefly overviews the advances in finite difference simulations, focusing particularly on earthquake mechanics and the resultant wave radiation in the near field. As the finite difference formulation is simple (interpolation is smooth), an easy coupling with other approaches is one of its advantages. A coupling with a boundary integral equation method (BIEM) allows us to simulate complex earthquake source processes.

1. Overview of finite difference approach in seismology

Seismic waves radiated from an earthquake propagate in the Earth, which is often considered as an elastic medium although the waves attenuate due to some anelasticity. The theory of wave propagation in an elastic medium was well established before the 20th century. In the early years of seismology, researchers tackled the relevant equations to obtain analytical (or semi-analytical) solutions [1]. These solutions are usually limited to some simple structures (e.g. 1D-layered model without any lateral medium heterogeneity). These solutions, however, are still useful as seismologists need a simple solution to rapidly analyse earthquakes. The advances in computing environments allowed the direct evaluation of the differential equation in the 1970s [2]. Since the mid-1990s, seismologists have been able to routinely carry out huge computations for various applications [3].

Let us consider a 3D isotropic elastic medium, characterized by two elastic (Lamé) coefficients λ and μ and density ρ. We denote displacement, velocity and stress as u, v, and τ, respectively. Taking a Cartesian coordinate (x, y, z), the equations of motion are written as

$$\rho \frac{\partial^2}{\partial t^2} u_i = \frac{\partial}{\partial x_j} \tau_{ij} + F_i$$

where indices represent each component or direction in the coordinates, and the summation convention about the same index is assumed. F is a body force (usually zero except for a particular source). The strain is defined as

$$\varepsilon_{ij} = \frac{1}{2}\left(\frac{\partial u_i}{\partial x_j} + \frac{\partial u_j}{\partial x_i} \right).$$

The constitutive relation between the stress and the strain is

$$\tau_{ij} = c_{ijkl}\varepsilon_{kl}$$

and

$$c_{ijkl} = \lambda\delta_{ij}\delta_{kl} + \mu(\delta_{ik}\delta_{jl} + \delta_{il}\delta_{jk})$$

where $\delta_{ij} = 1$ if $i = j$, otherwise 0. The differential equations of the seismic wave propagation consist of

$$\rho\frac{\partial}{\partial t}v_x = \frac{\partial}{\partial x}\tau_{xx} + \frac{\partial}{\partial y}\tau_{xy} + \frac{\partial}{\partial z}\tau_{xz} + F_x \text{ and two other equations.}$$

and

$$\frac{\partial}{\partial t}\tau_{xx} = \lambda\left(\frac{\partial}{\partial x}v_x + \frac{\partial}{\partial y}v_y + \frac{\partial}{\partial z}v_z \right) + 2\mu\frac{\partial}{\partial x}v_x \text{ and five other equations.}$$

This is called the stress-velocity formulation, for which it is easy to discretize the differential terms. For reasons of space, we have shown only one equation for each component of velocity and stress.

As for many other differential equations, various approximations of these equations are possible. However, the staggered-grid discretization in space and time is common for good stability [4]. Figure 1 shows the spatial definition of each component of velocity and stress, noting that each component is separated from the others by half a grid step (except for the diagonal component of stress). Stress and velocity are evaluated at different time steps (by half a time step). Recently partially-staggered grids were proposed [5] to combine all the stress components at one point and all the velocity components at another point separated by half a grid step. Such a modified method gives a better estimation of the boundary conditions, but additional operations are necessary. In many cases, the 4th order approximation on the spatial differential operator is adopted because of its efficiency;

$$\frac{\partial}{\partial x}f(x) = \frac{1}{h}\left(\frac{9}{8}\left\{ f(x+\frac{h}{2}) - f(x-\frac{h}{2}) \right\} - \frac{1}{24}\left\{ f(x+\frac{3}{2}h) + f(x-\frac{3}{2}h) \right\} \right).$$

Note that a time step is taken as $\Delta t \le c \cdot \Delta s / V_{\max}$ and the upper frequency limit is conventionally $f_{\max} = V_{\min}/(5\ \Delta s)$, where $V_{\max}$ and $V_{\min}$ are the maximum and minimum wave velocities in the modeled structure, respectively and Δt and Δs are the time step and grid spacing. The constant c is often taken to be about 0.5.

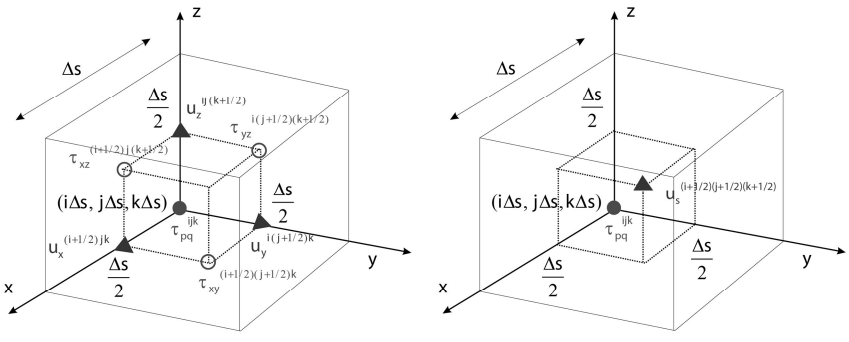

Figure 1: Illustration of standard staggered grid and partially-staggered-grid. The denoted components are defined half a grid apart from the others. For simplicity, equal grid size is taken for all the directions.

Seismologists often treat a finite volume extracted from the Earth for a regional problem (e.g. a cube of 100 x 100 x 50 km from a sphere of radius 6 400 km). Therefore, we should not have any artificial reflections from the given model boundaries, which should continue propagating outwards. For this purpose, an absorbing condition is required as a boundary to eliminate the reflected waves or a boundary zone absorbing the seismic waves [6]. Appropriate absorbing boundary conditions over a wide range of frequencies allow proper calculation not only of the wave propagation phase but also the residual displacement field. This feature becomes important when seismologists are interested in geodetic deformation of very long periods as well as short-period ground motions.

Figure 2 shows a simulation example of the wave propagation during the M9 2011 Tohoku-oki, Japan, earthquake, which was extremely large (a few hundred kilometers of fault length and more than a hundred seconds of rupture duration). High-sampling (1 Hz) continuous GPS observed the deformation process in displacement. We aim to reproduce such deformations without losing information on the residual absolute displacement, which is difficult to obtain from accelerometric data because of sensor response and low-frequency noise. In Figure 2, we show two finite difference simulations low-pass filtered (cut-off at 50 s); one is properly calibrated to use an absorbing boundary condition (FDM1), while the other, using the same code, is not (FDM2). We compare with the reference solution synthetically calculated with the wave-number method in the same 1D structure. We observe that FDM1 provides a reasonable solution compared to the reference solution including the residual displacement, while FDM2 has some bias. We note that both finite difference simulations are consistent in a band-pass filter range (1 to 10 s), so that the difference comes from the response at long periods. In fact, FDM1 is calibrated in its absorbing condition so as to work better at around a period of 100 s, while FDM2 is our conventional simulation of wave propagation adopted for a period of 1 s. This discrepancy is important to understand when applying finite difference schemes for long-period deformation processes. The simulations do not perfectly match the observations because of the use of a simple source model with very few parameters, but these simulations are good enough as a first-order approximation.

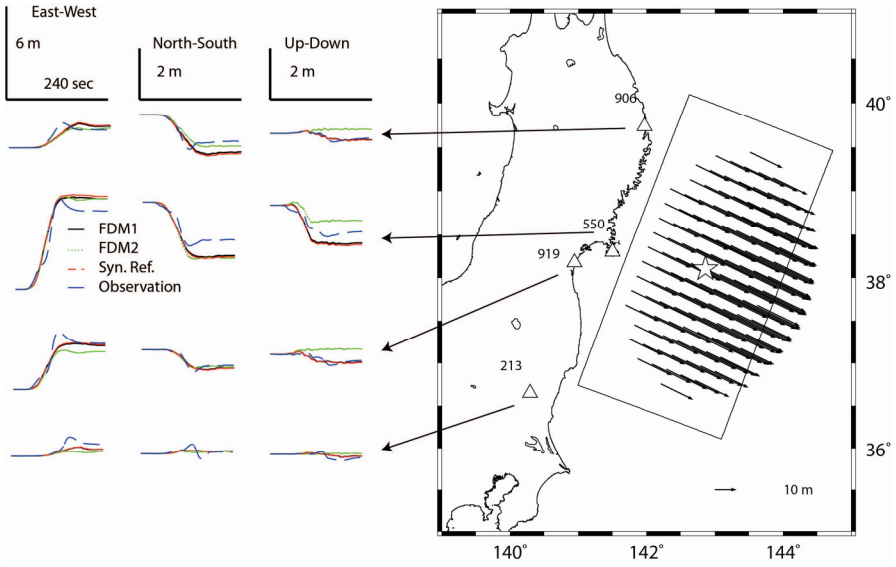

Figure 2: Finite difference simulation of wave propagation for the 2011 Tohoku-oki earthquake. A simple source model (a huge ellipse with Gaussian slip distribution and a constant rupture speed) is assumed (Madariaga, pers. comm. 2012). The waveforms (deformation) applied with a low-pass filter at 50 s are shown at four GPS stations. FDM1: Absorbing boundary condition is adapted for a period of 100 s, FDM2: the same code in the same condition except for the absorbing boundary condition calibrated for a conventional seismological frequency range of 1 s. Syn. Ref.: Synthetic reference solution calculated with a discrete wavenumber method in the same 1D layered structure. Observation: displacement record observed by high-sampling (1Hz) continuous GPS network of the Geographical Survey of Japan.

Other aspects, such as implementation of earthquake sources, treatment of the ground surface and material contrast are found in various studies [7]. The extensions to visco-elastic medium are given in [8]. The finite difference scheme has been generally developed for equally-spaced structural grids, so that it is rather easy to manage memory allocation in parallel computing. However it is possible to mix different grids or even combine with finite element grids [9]. From their early era of development, finite difference methods are used to apply a Message Passing Interface (MPI). This is necessary to reduce the unbalances between CPUs. New approaches using graphic card as well as the usual CPU (GPU-CPU) have been recently developed [10].

2. Earthquake physics and ground motion

2.1. Coupling with a boundary integral equation method

The finite difference scheme always has difficulty in treating dislocations (earthquake faulting) in the medium, although some improvement is possible [11]. The reason why this is difficult is that the dislocation problem is a discontinuous phenomenon in the continuum medium, governed by nonlinearity (fracture mechanics). Nevertheless, there is no problem in calculating wave propagation for any known sources within the proper frequency range. The convenient and practical solution is to combine it with other methods, in particular with a boundary integral equation (boundary element) method specialized for the dislocation [12]. Figure 3 shows the schematic illustration of the simulation procedure. In the following session, we present a study on the rupture dynamics and wave propagation in the very-near-field of an earthquake.

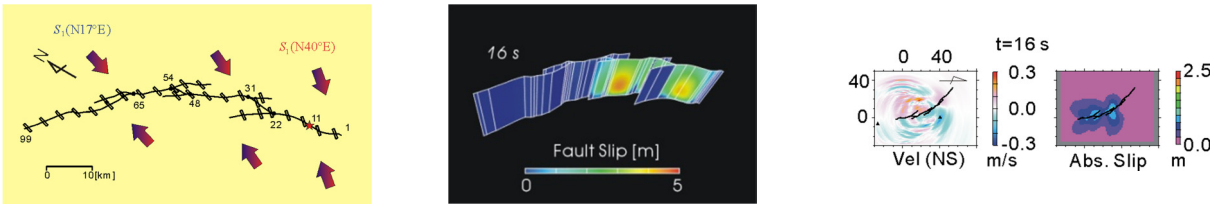

A: Initial Condition

B: Dynamic rupture process (boundary integral equation)

C: Near-field ground motion (finite difference simulation)

Figure 3: simulation strategy of earthquake dynamics to wave propagation starting from the physical and geological initial condition (A), using a boundary integral equation (B) and a finite difference method (C). The shown example is the case of the Mw7.3 1992 Landers earthquake [13].

2.2. Very-near-field ground motion

2.2.1. *Unresolved scientific problems.* Nowadays, seismologists are able to describe the earthquake rupture phenomena by kinematics in order to explain the regional or teleseismic data set (kinematic inversion). In other words, the regional seismic wave propagation (say at more than 10 km in a low frequency range below 0.5 – 1 Hz) is reasonably comprehensible. However, some observations very close to the causal fault (those leading to significant structural damage) can be somewhat unexpected. Although it is considered that these mechanisms are related to the dynamic rupture process of the causal fault, each case is not yet well resolved. The 2008 Mw6.9 Iwate-Miyagi, Japan, earthquake is remembered for the maximum recorded acceleration of 3800 cm/s^2 at the surface sensors of the station IWTH25 (Kik-net, NIED) located above the ruptured thrust fault (Figure 4). An acceleration of more than 1000 cm/s^2 is observed even at the borehole sensor (280 m depth) at the same station. The PGV also reaches about 100 cm/s. We focus on the fact that an extreme ground motion is found even at depth, and this should have originated from the source process. In particular, the PGV is found at the very beginning of the ground motions, about 2 seconds after the arrival of S wave, as the first main pulse.

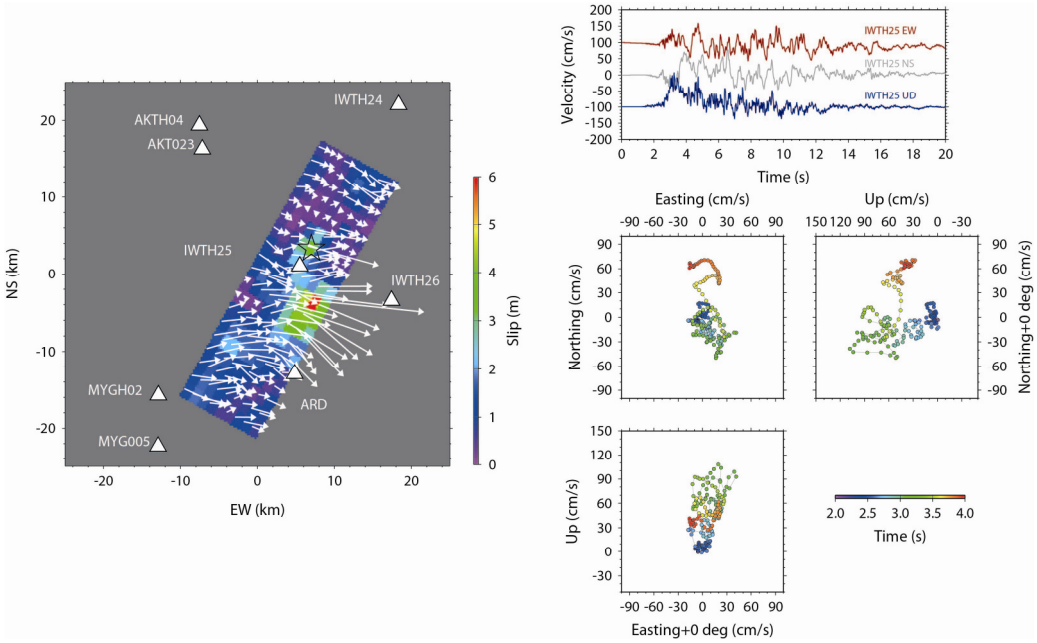

Figure 4: Map of the fault model (courtesy of Dr. Asano [14], slip distribution in color with arrows) of the 2008 Miyagi-Iwate earthquake in the left panel. Epicenter is shown as a star. A seismograph station, IWTH25, is located above the fault plane and close to the estimated epicenter, and this station recorded the very strong ground motions (100 cm/s) as shown in the right panel. The three components recorded at borehole (260 m depth) and the trajectory between 2 and 4 seconds, the arrival of the strong pulse, are shown. Very strong vertical motion is recorded at around 3.5 second.

2.2.2. *Kinematic and dynamic source process and wave radiation.* We compute the wave propagation from the published kinematic source models using a finite difference method. The 1D structure is assumed. We aim to calculate up to 2 Hz. We first model the ground motion based on the rupture scenario obtained from the kinematic inversion [14] (Fault strike = N201°E, dip = 51°, focal depth = 7.77 km). As already pointed out [15], mainly because of the resolution limit of the inversion model (subfaults of 2 km), the strong first pulse is hardly reproduced in terms of its huge amplitude and short duration. This infers that a heterogeneity equivalent or smaller than this scale may be important. Then we try to simulate the beginning of the rupture process (about the first 3 s). We investigate kinematically the effect of a small circular patch (radius = 1 km) on the ground motion at IWTH25 by shifting its location. For the given geometrical situation, it is found that a patch not located beneath the station, but slightly shallower (2 km away from the hypocentral depth) can give a relatively significant fault parallel (e.g. significant vertical) component in the ground motion, but no model leads to a perfect match to the observations.

We then try to model the rupture process dynamically supposing not the kinematic scenario but the physical parameters (stress field and rupture criterion). We assume a uniform shear stress field (5 MPa) except for a patch representing heterogeneity (if any) as demonstrated in Figure 2. A simple slip-weakening law is assumed (peak strength = 10 MPa, residual stress = 0 MPa, critical slip displacement = 5cm). Introducing a patch with higher initial stress generates heterogeneity in the rupture process. On the patch, the rupture passes locally faster than in other locations and leads to larger slip. We calculate the ground motion from this source model again, as shown in Figure 5, in which, for reference, the case of uniform dynamic rupture (without the patch) and the kinematic source model are also shown. The synthetic seismograms still have a smoother waveform regardless of the heterogeneity. The ground motion is a convolution over the fault plane, so the rupture propagation on the rest of the fault plane other than the given small patch affects it. We encounter two difficulties. The station is unfavorably located with respect to the S-wave radiation from the assumed fault plane, and it is difficult to give the dynamic model a strong heterogeneity at the beginning without

significantly affecting the later rupture process. As recent geodetic studies imply [16], the true fault geometry may not be as simple as a single fault.

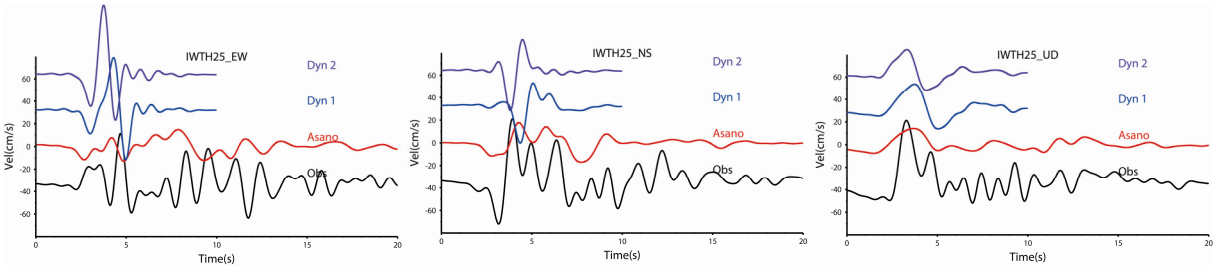

Figure 5: Comparison of seismograms (low-pass filtered at 1 Hz) at IWTH25 at depth for various source models. The calculation is made by the finite difference method using a 1D structure model beneath IWTH25. From top to down, dynamic rupture model presented with heterogeneity, dynamic rupture model under the homogeneous condition, kinematic rupture model of Asano and Iwata (2008), and the observation. For the three synthetic models, the origin time is set at t=0. Because of uncertainty in the real origin time, the observation may be shifted in time. The dynamic rupture model provides a shaper pulse, but no model can explain the pulse of the first two seconds.

2.2.3. *Discussion – do we really know the earthquake process?* In fact, we have been trying to simulate the recent earthquakes according to the known parameters (source parameters and structure) [17]. We think that such reproduction process is important, because predicting the ground motion in any given situation is the objective of the quantitative seismic hazard assessment. From our several experiences, we find that the "known" parameters are not always satisfactory to explain the phenomena. This is because the earthquake process is too complex to determine all the numerous parameters necessary to construct the models. Any parameter is obtained under some hypothesis, e.g., fixing the other parameters. This is also why inversion analyses sometimes provide different models even using the same data set.

The seismology (and also the other domains of geoscience) is always in a knowledge gap; we try to model more precisely the phenomena using any numerical sophisticated method and intensive calculation (forward modeling), while the model parameters are not acquired precisely enough regardless of the increase of high-quality various data (inverse modeling). The sustainable efforts to fill in this gap are required, since this cannot be done easily. The intensive numerical simulation will be able to be a powerful tool towards this objective.

3. Perspectives and Conclusion

Nowadays, when the accuracy of the calculation is aimed, higher-order finite element methods (spectral element or discontinuous Galerkin) could be better regardless of their costs [18]. Each method always has its merits and limits so that it is waited that various methods are developed and utilized. Such numerical codes have become also popular for engineering/industrial purpose such as the quantitative seismic hazard/risk assessments [19], however guaranteeing the numerical performance on parallel computers and obtaining the physically reasonable solutions are difficult tasks. Since 2000, various international benchmark and cross-checking tests have been also performed [20]. This is necessary for us to advance beyond.

The finite difference formulation for the seismic wave propagation is the most primary scheme. However, this always shows a good (computing) performance and this is often satisfactory for tackling the unsolved physical problems, as shown briefly in this paper. The basic formulation of finite difference is very well established and we can relatively easily handle the intensive calculation. Thus making full use of it, we are now able to explore the earthquake dynamics and the consequent ground motion. Coupling with a boundary integral equation is a practical option to take advantage of both

methods. At the end, we precise that the finite difference scheme is classical, but the formulation always evolves for improving solutions and developing for other utilities [21].

Acknowledgments

This paper is a contribution to the French national project ANR DYNTOHOKU. Most of the recent numerical simulations are carried out at the French national computing center GENCI-CINES (grant 2012-46700), but some other results realised in previous projects are also included (BRGM-ANR-CARNOT). The data recorded by National Institute of Earth Science and Disaster Prevention, Japan (strong ground motion) and Geographical Institute of Japan (GPS) are used.

References

[1] Aki, K. and P. Richards (2002), Quantitative seismology, 2nd edition, University Science Books.

[2] Boore, D. M. (1972), Finite difference methods for seismic wave propagation in heterogeneous materials, in Methods in Computational Physics, Academic Press, 1-37.

Madariaga, R. (1976), Dynamics of an expanding circular fault, Bull. Seism. Soc. 66, 639-666.

[3] Olsen, K. B., Archuleta, R. J. and J. Matarese (1995), Three-dimensional simulation of a magnitude 7.75 earthquake on the San Andreas fault, Science, 270, 1628-1632.

Furumura, T. and L. Chen (2004), Large scale parallel simulation and visualization of 3D seismic wavefield using the Earth Simulator, Comp. Model. Eng. Sci., 6, 153-168.

[4] Virieux, J. and R. Madariaga (1982), Dynamic faulting studied by a finite difference method, Bull. Seism. Soc. Am., 72, 345-369.

[5] Saenger, E. H., N. Gold and S. A. Shapiro (2000), Modeling the propagation of elastic wave waves using a modified finite-difference grid, Wave Motion, 31, 77-92.

[6] Clayton, R. and B. Engquist (1977), Absorbing boundary conditions for acoustic and elastic wave equations, Bull. Seism. Soc. Am., 67, 1529-1540.

Collino, F. and C. Tsogka (2001), Application of the perfectly matched absorbing layer model to the linear elastodynamic problem in anisotropic heterogeneous media, Geophysics, 66, 294-307.

Komatitsch, D. and R. Martin (2007), An unsplit convolutional perfectly matched layer improved at grazing incidence for the seismic wave equation, Geophysics, 72, SM155-167.

[7] Graves (1996), Simulating seismic wave propagation in 3D elastic media using staggered-grid finite differences, Bull. Seism. Soc. Am., 86, 1091-1106.

Mozco, P., J. Kristek, M. Galis, P. Pazak and M. Balazovjech (2007), The finite-difference and finite-element modeling of seismic wave propagation and earthquake motion, Acta Physica Slovaca, 57, 177-406.

[8] Day, S. M. and C. Bradley (2001), Memory-efficient simulation of anelastic wave propagation, Bull. Seism. Soc. Am., 91, 520-531.

Kristek, J. and P. Moczo (2003), Seismic-wave propagation in viscoelastic media with materialdiscontinuities: A 3D fourth-order staggered-grid finite-difference modeling, Bull. Seism. Soc. AM., 93, 2273-2280.

[9] Aoi, S. and H. Fujiwara (1999), 3-D finite-difference method using discontinuous grids, Bull. Seism. Soc. Am., 89, 918-930.

Ducellier, A. and H. Aochi (2012), Effects of the interaction of topographic irregularities on seismic ground motion, investigated by the hybrid FD-FE method, Bull. Earthq. Eng., 10, 773-792

[10] Dupros, F., H. Aochi, A. Ducellier, D. Komatitsch and J. Roman (2008), Exploiting intensive multithreading for efficient simulaton of seismic wave propagation, 11th Int. Conf. Computational Science and Engineering, 253-260, doi:10.1109/CSE.2008.51.

Michéa, D. and D. Komatitsch (2010), Accelerating a 3D finite-difference wave propagation code using GPU graphics cards, Geophys. J. Int., 182, 389-402.

[11] Cruz-Atienza, V. M., J. Virieux and H. Aochi (2007), 3D finite-difference dynamic-rupture modeling along nonplanar faults, Geophysics, 72, SM123-137.
Dalguer, L. A. and S. M. Day (2007), Staggered-grid split-node method for spontaneous rupture simulation, J. Geophys. Res., 112, B02302, doi:10.1029/2006JB004467.
[12] Aochi, H. and R. Madariaga (2003), The 1999 Izmit, Turkey, earthquake: Nonplanar fault structure, dynamic rupture process, and strong ground motion, Bull. Seism. Soc. Am., 93, 1249-1266.
Fukuyama, E., R. Ando, C. Hashimoto, S. Aoi and M. Matsu'ura (2009), Physics-based simulation of the 2003 Tokachi-oki, Japan, earthquake to predict strong ground motions, Bull. Seism. Soc. Am., 99, 3150-3171.
[13] Aochi, H., E. Fukuyama and R. Madariaga (2003), Constraints of fault constitutive parameters inferred from non-planar fault modeling, Geochemistry, Geophysics, Geosystems, 4, doi:10.1029/2001GC000207.
[14] Asano, K. and T. Iwata (2008), Kinematic source rupture process of the 2008 Iwate-Miyagi Nairiku earthquake, a Mw6.9 thrust earthquake in northeast Japan, using Strong Motion Data, EOS Trans. Am. Geophys. Union, 89(53), Fall Meeting Suppl. Abstract S23B-1890.
[15] Suzuki, W., S. Aoi and H. Sekiguchi (2010), Rupture process of the 2008 Iwate-Miyagi Nairiku, Japan, earthquake derived from near-source strong-motion records, Bull. Seism. Soc. Am., 100, 256-266.
[16] Takada, Y., T. Kobayashi, M. Furuya and M. Murakami (2011), Post-seismic surface deformation following the 2008 Iwate-Miyagi Nairiku earthquake detected by ALOS/PALSAR, J. Geod. Soc. Jpn., 57, 181-193.
[17] Aochi, H., V. Durand and J. Douglas (2011), Influence of super-shear earthquake rupture models on simulated near-source ground motion from the 1999 Izmit (Turkey) earthquake, Bull. Seism. Soc. Am., 101, 726-741.
Aochi, H., A. Ducellier, F. Dupros, M. Delatre, T. Ulrich, F. de Martin and M. Yoshimi (2011), Finite difference simulations of the seismic wave propagation for the 2007 Mw6.6 Niigata-ken Chuetsu-oki earthquake : Validity of models and reliable input ground motion in the near field, Pure appl. Geophys., doi:10.1007/s00024-011-0429-5.
[18] Komatitsch, D. and J. P. Vilotte (1998), The spectral-element method: An efficient tool to simulate the seismic response of 2D and 3D geological structures, Bull. Seism. Soc. Am., 88, 368-392.
Chaljub, E., D. Komatitsch, J. Vilotte, Y. Capdeville, B. Valette, and G. Festa (2007), Spectral element analysis in seismology, in "Advances in wave propagation in heterogeneous media, Advances in Geophysics", Elsevier Academic Press, 365-419.
Dumbser, M. and M. Käser (2006), An arbitrary high-order discontinuous Galerkin method for elastic waves on unstructured meshes – II. The three-dimensional isotropic case, Geophys. J. Int., 167, 319-336.
Etienne, V., E. Chaljub, J. Virieux and N. Glinsky (2010), An hp-adaptive Galerkin finite-element method for 3D elastic wave modelling, Geophys. J. Int.,183, 941-962.
De Martin, F., Verification of a spectral-element method code for the Southern California Earthquake Center LOH.3 Viscoeastic case, Bull. Seism. Soc. Am., 101, 2855-2865.
[19] Douglas, J. and H. Aochi (2008), A survey of techniques for predicting earthquake ground motions for engineering purposes, Survey in Geophysics, 29, 187-220.
[20] Day, S. M., J. Bielak, D. Dreger, R. Graves, S. Larsen, K. B. Olsen and A. Pitarka (2001), Tests of 3D elastodynamic odes: final report for lifelines project 1A01, report to Pacific Earthquake Engineering Research Center.
Chaljub, E., P. Moczo, S. Tsuno, P.-Y. Bard, J. Kristek, M. Käser, M. Stupazzini and M. Kristekova (2010), Quantitative comparison of four numerical predicsions of 3D ground motion in the Grenoble Valley, France, Bull. Seism. Soc. Am., 100, 1428-1455.
Harris, R. A., M. Barell , D. J. Andrews, B. Duan, S. Ma, E. M. Dunham, A.-A. Gabriel, Y.

Kaneko, Y. Kase, B. T. Aagaard, D. D. Oglesby, J.-P. Ampuero, T. C. Hanks and N. Abrahamson (2011) Verifying a compuational method for predicting extreme ground motion, 82, 638-644.

[21] Kozdon, J. E., E. M. Dunham and J. Nordstrom (2012), Simulation of dynamic earthquake ruptures in complex geometries using high-order finite difference methods, J. Scientific Computing, doi:10.1007/s10915-012-9624-5.

Zhang, W., Z. Zhang an X. Chen (2012), Three-dimensional elastic wave numerical modelling in the presence of surface topography by a collocated-grid finite-difference method on curvilinear grids, Geophys. J. Int., 190, 358-378.